DOI: 10.1111/mice.13144

RESEARCH ARTICLE

COMPUTER-AIDED CIVIL AND INFRASTRUCTURE ENGINEERING WILEY

Field-tested signal controller to mitigate spillover using trajectory data

Yu Han[1] | Zhe Han[1] | Fan Ding[1] | Fuliang Li[2] | Hao Wang[1] | Xingmin Wang[3]

[1]School of Transportation, Southeast University, Nanjing, China

[2]Department of Electrical Engineering, The Hong Kong Polytechnic University, Hung Hom, Kowloon, Hong Kong, China

[3]Department of Civil and Environmental Engineering, University of Michigan, Ann Arbor, Michigan, USA

Correspondence
Hao Wang, School of Transportation, Southeast University, Nanjing, China.
Email: haowang@seu.edu.cn

Xingmin Wang, Department of Civil and Environmental Engineering, University of Michigan, Ann Arbor, MI, USA.
Email: xingminw@umich.edu

Funding information
National Key Research and Development Program of China, Grant/Award Number: 2022ZD0115600; National Natural Science Foundation of China, Grant/Award Numbers: 52002065, 52131203

Abstract

Trajectory data from connected vehicles (CVs) provide a continuous and reliable means of obtaining information that can be leveraged to optimize traffic signals. This paper proposes a real-time traffic signal control method using CV trajectory data as the sole input. The primary goal of the proposed signal control method is to prevent queue spillover, which may significantly decrease the traffic efficiency on urban networks and induce high delays to the travelers. The proposed method formulates the signal control problem via a linear quadratic optimization model, considering the constraints related to the duration and variability of green lights in practical traffic signal control systems. Compared to conventional max-pressure-based methods, the optimization model offers enhanced efficiency in handling these constraints, making it highly suitable for real-life implementation. The proposed method has undergone testing in both simulated environments and real-world applications. In the simulation experiments, the proposed method has been demonstrated to effectively reduce spillover risks and outperform a conventional max-pressure-based approach even when the CV penetration rate is as low as 5%. In the real-world experiment, the proposed method had been tested in a traffic network around the Beijing Capital International Airport for several months. The severity of spillovers, which was represented by two performance indicators, had been significantly reduced after implementing the proposed method.

1 | INTRODUCTION

Urban traffic control (UTC) has emerged as a prominent research focus in transportation engineering due to its direct impact on people's daily lives. Ineffective control strategies can diminish roadway capacity, resulting in increased travel delays and potential safety risks. During peak hours, when urban traffic networks experience over-saturation, the primary objective of UTC is to prevent spillover (Papageorgiou et al., 2003). Spillover refers to the phenomenon where growing queues extend to the upstream of roadway links, obstructing the arrival flow from upstream intersections (Geroliminis & Sun, 2011). This reduction in throughput at the upstream intersection may propagate to further upstream and even result in gridlock (Daganzo, 1998). Therefore, preventing spillovers is crucial for effectively implementing UTC.

Queue spillovers can be prevented by regulating the inflows and outflows of the overlong queues via optimizing the signals of the direct upstream and downstream intersections. Conventional signal control systems like SCOOT (Hunt et al., 1982) and SCATS (Lowrie, 1982), which are primarily designed for under-saturated traffic conditions, become ineffective in addressing spillovers that occur during over-saturated traffic conditions. The recent literature on advanced traffic signal control methods can be categorized into three main groups: (i) model-based optimal control methods, (ii) reinforcement learning (RL)-based methods, and (iii) back-pressure-based methods. These categories provide different approaches for tackling the challenge of traffic signal control.

Existing model-based methods for traffic signal control have been developed based on different traffic flow models, including store-and-forward models (Le et al., 2013), discrete first-order models (Han et al., 2018), high-order models (Van den Berg et al., 2007), and macroscopic fundamental diagram (MFD; Geroliminis et al., 2012). Since model-based optimizations usually suffer from high computational loads, the scalability and real-time application for most of those methods remain challenging. Furthermore, the performance of a model-based traffic controller is hindered by discrepancies between the traffic prediction model and the actual traffic dynamics, leading to suboptimal outcomes.

RL-based traffic signal control methods have attracted significant attention over the past few years. While many existing RL-based traffic signal control methods are model-free and do not require a model to reproduce traffic state transitions during training, they still rely on a traffic simulator for the training process. The performance of RL-based strategies can be limited by the discrepancy between a traffic simulator and the actual traffic process. Moreover, the training processes of these RL models cannot be conducted in the real world due to the random exploration of new control actions, which often leads to significant costs in terms of delays caused by exploration and learning. Consequently, implementing these RL-based traffic signal control strategies in the field is not straightforward until the aforementioned challenges are overcome (Han et al., 2023).

The max-pressure (or back-pressure) algorithms were initially applied to an isolated intersection signal control method proposed by Wunderlich et al. (2007) and to network-wide signal control by Wongpiromsarn et al. (2012) and Varaiya (2013). It provides a scalable control policy, where each intersection makes its own decisions by considering the queue lengths of vehicles both upstream and downstream. The original back-pressure algorithm has been extended in several aspects. For instance, the assumption of infinite link capacity in the original algorithm has been addressed in studies by (Gregoire et al., 2014; L. Li & Jabari, 2019), which consider bounded queue constraints and the propagation of shockwaves. The original back-pressure algorithm applied a fixed cycle control policy, that is, activating the phase with the maximum weight in a fixed time slot, which is also undesirable since erratic ordering of phases brings frustration to drivers. The methods (Le et al., 2015; Levin et al., 2020) applied "cyclic phases" policy that arranges the phases into a fixed-ordered sequence. In recent studies, the back-pressure approach has been combined with model-based optimal control methods or RL methods (D. Ma et al., 2020; Wang et al., 2022). A summary of significant publications on max-pressure methods is presented in Table 1.

Most of the aforementioned traffic signal control strategies did not explicitly consider mitigating spillover, although by reducing delays, the risk of spillover may also be reduced. Furthermore, while advanced traffic signal control strategies have demonstrated their effectiveness in alleviating congestion and reducing delays in simulations, their practical implementation remains limited. Max-pressure approaches offer distinct advantages over model-based approaches and RL approaches in terms of their feasibility for field implementation. One notable advantage is their low computational burden, which is particularly advantageous for real-time traffic control. Furthermore, these approaches only rely on observation, without requiring any traffic flow model or predictions. Nevertheless, despite these benefits, the widespread adoption of max-pressure approaches in the field has been limited, with only a few successful implementations to date. Only two studies conducted field test experiments to evaluate their respective back-pressure approaches (Levin, 2023). Mercader et al. (2020) implemented a back-pressure method based on travel time data measured from Bluetooth detectors at an intersection in Jerusalem. The experiment reported a 4% reduction in normalized travel time. Dixit et al. (2020) implemented a back-pressure method in seven intersections across India and Indonesia, using crowdsourced travel time data from Google Maps. The results indicated a decrease in travel delays at all intersections.

The challenges for implementing traffic signal control methods in real-world settings encompass various factors beyond the aforementioned computational efficiency and model mismatch problems. First, the operation of practical adaptive signal control systems often depends on the data collected from fixed sensors, such as loop detectors. However, the sensor failures in those systems can significantly affect the control performance. Additionally, the data collected from loop detectors, including traffic counts and occupancy at specific locations, cannot be directly used to model and optimize delays and queue lengths in urban traffic. Second, practical traffic signal control systems operate with various constraints that are often overlooked by

TABLE 1 A summary of significant publications on max-pressure methods.

Paper	Cycle mode	Traffic state input	Testing environment	Key achievement
Wunderlich et al. (2007)	Acyclic	Accurate queue length	VISSIM	First applied max-pressure concept to an isolated intersection
Wongpiromsarn et al. (2012)	Acyclic	Accurate queue length	MITSIMLab	One of the first to apply max-pressure algorithm to network signal control
Varaiya (2013)	Acyclic	Queue length with measurement errors	N/A	One of the first to apply max-pressure algorithm to network signal control
Gregoire et al. (2014)	Acyclic	Accurate queue length	SUMO	Considered bounded queue constraints in pressure calculation
Le et al. (2015)	Cyclic	Accurate queue length	SUMO	First proposed cycle-based max-pressure control algorithm
Xiao et al. (2015)	Cyclic	Queue length with measurement errors	VISSIM	Considered optimized traffic signals in different traffic flow situations by tuning the control parameters
L. Li and Jabari (2019)	Acyclic	Queue length with measurement errors	SCOOT	Considered the propagation of shockwaves
Wei et al. (2019)	Acyclic	Accurate queue length	CityFlow	Combined max-pressure control method with reinforcement learning
Dixit et al. (2020)	Cyclic	Travel time data obtained from Google Maps	Field test in seven intersections across India and Indonesia	Conducted field test experiment
Levin et al. (2020)	Cyclic	Accurate queue length	Numerical simulation	Incorporated max-pressure control method into a model predictive controller
Mercader et al. (2020)	Cyclic	Travel time data measured from Bluetooth detectors	Field test at an intersection in Jerusalem	Conducted field test experiment

existing methods. For instance, these systems commonly employ the fixed cyclic phase mode, where the green of each phase must satisfy a minimum value to ensure pedestrian safety. Furthermore, in order to maintain the stability of traffic flow, it is necessary to impose limits on the variability of green duration between consecutive cycles. The complexity of signal control systems, which encompass numerous phases and multiple constraints for each phase, poses a significant challenge for conventional back-pressure methods in calculating an optimal signal plan that fulfills all the constraints. Last but not least, a common limitation in existing algorithms lies in their implicit treatment of real-time traffic state variables, such as queue lengths and delays, by assuming the availability of accurate traffic state, data as summarized in Table 1. While some studies have acknowledged the presence of errors in traffic state estimation, they often introduce artificial noise to the traffic state, neglecting practical traffic measurement and estimation considerations (Jiang & Adeli, 2004; Karim & Adeli, 2003). The integration of practical traffic measurement is a crucial factor for the successful deployment of traffic signal control methods in real-world applications.

The development of vehicle-to-everything (V2X) communication technologies has greatly enhanced the accessibility of trajectory data (Peng et al., 2021; Xu et al., 2022). This valuable data source provides a continuous and reliable means to obtain real-time traffic state information, which can be used for platoon control (D. Li et al., 2023; Shi, Nie, et al., 2022), bus control (Shi, Zhou, et al., 2022), and traffic signal control (Ding et al., 2022; C. Ma et al., 2023; Zhang et al., 2022). It is noteworthy that the two aforementioned successfully implemented back-pressure traffic signal control methods both relied on trajectory data. In this paper, we propose a real-time traffic signal control method that effectively prevents spillover by utilizing connected vehicle (CV) trajectory data as the sole input. The proposed method incorporates the idea of pressure, inspired by the back-pressure approach, to represent the difference in traffic loads of the upstream and downstream queues of a movement. To quantify the spillover risk of each movement, a spillover pressure is defined based on the estimated queue lengths of the upstream and downstream. To reduce the spillover risks, the signals are optimized to enlarge the outflow and reduce the inflow of the overlong queues. The signal control problem is tackled by formulating it as a computationally efficient linear quadratic optimization model. Furthermore, we incorporate additional constraints relevant to practical traffic signal control systems into the optimization model. The proposed method is tested in both simulations and practice. In the simulation experiments, the performance of the proposed method is assessed by comparing it with several baseline methods, which include a fixed-time control method and an existing back-pressure-based method. In the real-world experiment, the proposed method is implemented and evaluated in a traffic network consisting of 13 intersections. The evaluation of its performance is based on two performance indicators derived from CV trajectories collected before and after the implementation of the method.

The remaining sections of the paper are structured as follows. Section 2 introduces the control formulation of the proposed method. Section 3 and Section 4 present the simulation study and the real-world experiment, respectively. Section 5 concludes the paper with a summary of the findings and a discussion on future work.

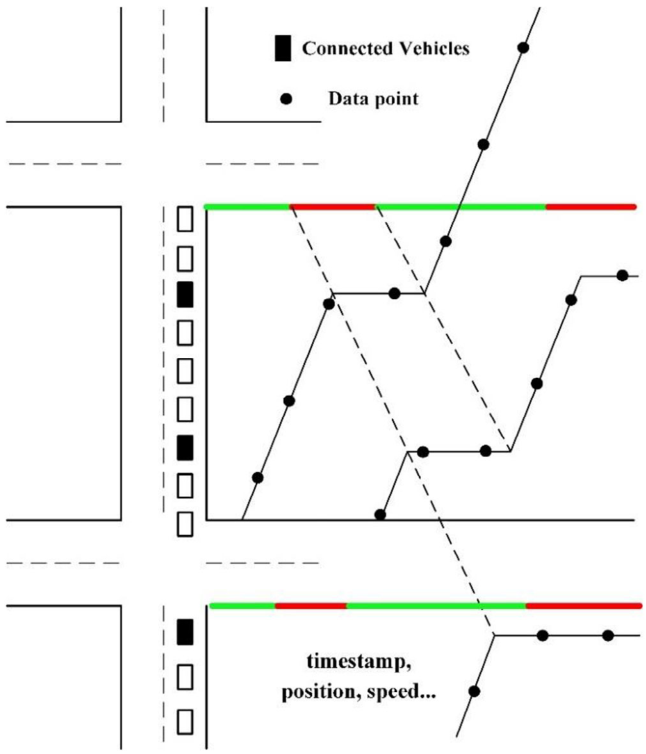

FIGURE 1 A schematic example of trajectory data from connected vehicles (CVs).

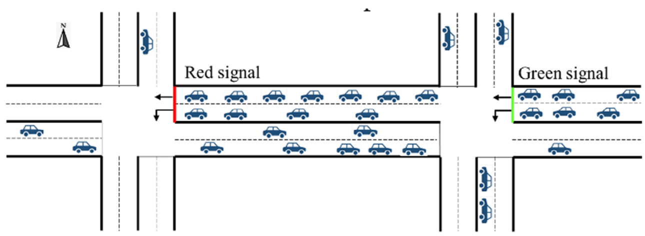

FIGURE 2 A schematic example of queue spillover.

2 | METHODOLOGY

This section presents the traffic signal control method for spillover dissipation. Section 2.1 briefly illustrates the CV trajectory data that are used for signal optimization. Section 2.2 presents the definition of variables in the signal control problem. Section 2.3 presents the formulation of the controller.

2.1 | Description of trajectory data

Trajectory data of CV refer to the comprehensive and granular information captured and recorded about the movement patterns and behaviors of vehicles equipped with communication capabilities. Figure 1 shows an example in which CV trajectories are collected from urban intersections. The block dots represent the data points, which include the position, speed, acceleration, and timestamp of each vehicle's location updates. The frequency of updates can range from a few seconds to a minute, depending on the system's requirements and the desired level of responsiveness. From this information, the traffic state of a roadway link, such as the travel time and queue length, can be estimated (Mei et al., 2019; Zhao et al., 2021).

2.2 | Definition of variables

As presented, a spillover occurs when a growing queue reaches the upstream end of the roadway link and blocks the arrival flow from the direct upstream intersection. Figure 2 shows an example of a spillover, which occurs at the east–west movement of the left intersection. As the queue reaches the upstream end of the link, traffic of the upstream movements is partially blocked even though the movements have the right of way. This causes a throughput reduction of the right intersection.

Let $\mathcal{G} = (\mathcal{N}, \mathcal{L})$ represent a traffic network that is composed of intersections $n \in \mathcal{N}$ and movements $m \in \mathcal{M}$. A movement is defined as a certain moving direction in the intersection; for example, a typical approach has three movements including the left-turn, right-turn, and through movements. For each intersection n, $\mathcal{M}_n^{\text{in}}$ is the set of entry movements into the intersection; $\mathcal{M}_m^{\text{out}}$ is the set of downstream movements of the upstream movement m.

In this paper, we assume that the intersection signals are operated with fixed cyclic phases. For the intersection n, the set of phases is represented by $\mathcal{P}_n$. A distributed traffic signal control method for fixed cyclic phases was proposed (Le et al., 2015). In that method, for intersection n, the weight for each upstream movement, $m \in \mathcal{M}_n^{\text{in}}$, was defined as

$$\omega_m(t) = c_m \cdot \left(x_m(t) - \sum_{m' \in \mathcal{M}_m^{\text{out}}} \gamma_{mm'}(t)\, x_{m'}(t) \right) \tag{1}$$

where c_m is the saturation flow rate of movement m. $x_m(t)$ is the number of vehicles in the upstream queue of the movement. $\gamma_{mm'}$ is the proportion of traffic from movement m that subsequently join the downstream movement $m' \in \mathcal{M}_m^{\text{out}}$ at time t. Let $\mathcal{M}_p^n$ be the set of movements controlled by phase p; vehicles of these movements are allowed to pass the intersection during phase p. The weight for phase p at time t is defined as the addition of the movement weight:

$$w_p(t) = \sum_{m \in \mathcal{M}_p^n} \omega_m(t) \tag{2}$$

$$g_p(k) = G(k) \cdot \frac{\exp\left(\phi \cdot w_p(k)\right)}{\sum_p \exp\left(\phi \cdot w_p(k)\right)} \tag{3}$$

where $G(k)$ is the total green duration of cycle k. $w_p(k)$ is the weight of phase p at the beginning of cycle k. ϕ is a model parameter shown in Table 2.

The aforementioned traffic signal control method (which is referred to as Le's method in the rest of the paper) distributes the total green time of each cycle based on the weight of each movement, that is, the difference in traffic loads between the upstream and downstream, which is similar to the concept of pressure in the well-known back-pressure algorithm (Varaiya, 2013; Wongpiromsarn et al., 2012). However, a noticeable problem with Le's method is that it does not give priority to prevent spillovers. For example, if the queue length of a downstream movement m' is long but the turning fraction $r_{mm'}$ is small, the weight of movement m calculated based on Equation (1) may still be large. Under such a circumstance, the controller may give that movement a large green duration, resulting in a high arrival flow to the long queue, and consequently inducing a spillover.

To this end, we introduce a new weight function for each movement m to quantify the risk of spillover, which is defined as the following equations

$$r_m(t) = \begin{cases} \frac{l_m(t)}{L_m}, & l_m(t) \geq L_m \cdot r_c \\ 0, & l_m(t) < L_m \cdot r_c \end{cases} \tag{4}$$

where l_m is the distance between the position of the most upstream queuing vehicle and the stop bar for the upstream queue of movement m, and L_m is the length of the upstream link of movement m. r_c is a pre-determined threshold. The spillover risk is defined as the queue length occupation rate (abbreviated as queue length in the rest of the paper) if the queue length is larger than the threshold r_c; otherwise, the spillover risk will be 0.

The spillover pressure for movement $m \in \mathcal{M}_n^{\text{in}}$ is defined as

$$v_m(t) = \max_{m' \in \mathcal{M}_m^{\text{out}}} \{r_{m'}(t)\} - r_m(t) \tag{5}$$

which is the difference between the downstream spillover risk and the upstream spillover risk. The downstream spillover risk is used as the maximum spillover risk of all the downstream movements. According to the definition, $v_m(t) < 0$ when the upstream queue has a higher spillover risk, while $v_m(t) > 0$ when the downstream queues have a higher spillover risk.

For all the movements in phase p, the movement which has the maximum absolute value of the spillover pressure is defined as the critical movement, represented by m_{c},

$$m_{\text{c}}^p = \underset{m \in \mathcal{M}_p^n}{\operatorname{argmax}} \{|\, v_m(t)\, |\} \tag{6}$$

The spillover pressure for each phase p is represented by the spillover pressure of the critical movement, that is, $v_p(t) = v_{m_{\text{c}}^p}(t)$.

2.3 | Control formulation

Based on the defined spillover pressure, we develop a traffic signal controller to reduce the spillover risk. The exponential function of the spillover pressure is given by:

$$h_p(t) = \exp\left(\mu \cdot v_p(t)\right) \tag{7}$$

TABLE 2 Symbols of the variables and their explanations.

Symbol	Explanation
$\mathcal{M}_n^{\mathrm{in}}$	The set of entry movements into intersection n
$\mathcal{M}_m^{\mathrm{out}}$	The set of downstream movements of the upstream movement m
$\mathcal{P}_n$	The set of phases for intersection n
$\mathcal{M}_p^n$	The set of movements controlled by phase p
$\omega_m(t)$	The weight for movement m at time t
c_m	The saturation flow rate of movement m
$x_m(t)$	The number of vehicles in the upstream queue of the movement at time t
$\gamma_{mm'}(t)$	The proportion of traffic from movement m that joins the downstream movement m'
$w_p(t)$	The weight for phase p at time t
ϕ	A model parameter
$r_m(t)$	The weight of movement m, which quantifies the risk of spillover at time t
l_m	The queue length of movement m
L_m	Length of the upstream link of movement m
r_c	The pre-determined spillover threshold
$v_m(t)$	Difference between the downstream and the upstream spillover risk at time t
m_c^p	The critical movement in phase p
$v_p(t)$	The spillover pressure for each phase p at time t
$h_p(t)$	Exponential function of the spillover pressure for each phase p at time t
μ	A model parameter that is a large positive number
ϵ	A model parameter that is a small negative number
$Q_p(k)$	Total number of vehicles served during phase p in control cycle k
$g_p(k)$	Green duration of each phase p at cycle k
$G(k)$	Total effective green duration at cycle k
$g_p^{\min}$	The minimum green duration of phase p
$g_p^{\max}$	The maximum green duration of phase p
$\Delta g_p^{\max}$	The maximum variation of green duration between consecutive cycles for phase p

where μ is a large positive number. According to the definition of spillover pressure, for all the movements controlled by phase p, if the maximum spillover risk is higher than the maximum spillover risk of their downstream movements, $v_p(t) < 0$, and $h_p(t)$ is close to zero; if their downstream movements have a higher maximum spillover risk, $v_p(t) > 0$, and $h_p(t) > 1$; if all the movements and their downstream movements have no spillover risk, $v_p(t) = 0$, and $h_p(t) = 1$.

The green duration of each phase p at the start of cycle k, represented as $g_p(k)$, is given by the following linear quadratic optimizer:

$$\min \sum_p \left[\left(h_p(k) \cdot \frac{g_p(k)}{g_p(k-1)} \right)^2 + \epsilon Q_p(k-1) \cdot \frac{g_p(k)}{g_p(k-1)} \right] \tag{8}$$

subject to:

$$\sum^p g_p(k) = G(k) \tag{9}$$

$$g_p^{\min} \le g_p(k) \le g_p^{\max} \tag{10}$$

$$|g_p(k) - g_p(k-1)| \le \Delta g_p^{\max} \tag{11}$$

where $h_p(k)$ is the spillover pressure of phase p at the beginning of control cycle k. $g_p(k-1)$ is the green duration of phase p in control cycle $k-1$. $Q_p(k-1)$ is the total number of vehicles served during phase p in control cycle $k-1$. $g_p^{\min}$ and $g_p^{\max}$ denote the minimum and maximum green durations of phase p, respectively. $\Delta g_p^{\max}$ is the maximum variation of green duration between consecutive cycles. ϵ is a small negative number. The matrix form of the objective function can be written as

$$\min g(k)^T H(k) g(k) + \epsilon f(k-1)^T \cdot g(k) \tag{12}$$

where $g(k)$, $H(k)$, and $f(k-1)$ are defined as

$$g(k) = [g_1(k), \ldots, g_p(k), \ldots]^T \tag{13}$$

$$H(k) = \begin{bmatrix} \left(\frac{h_1(k)}{g_1(k-1)}\right)^2 & 0 & \cdots & 0 \\ 0 & \ddots & 0 & \vdots \\ \vdots & 0 & \left(\frac{h_p(k)}{g_p(k-1)}\right)^2 & 0 \\ 0 & 0 & 0 & \ddots \end{bmatrix} \tag{14}$$

$$f(k-1) = \left[\frac{Q_1(k-1)}{g_1(k-1)}, \ldots, \frac{Q_p(k-1)}{g_p(k-1)}, \ldots\right]^T \tag{15}$$

where in $f(k-1)$, $\frac{Q_p(k-1)}{g_p(k-1)}$ denotes the average flow rate of phase p in control cycle $k-1$. In Equation (11), H is positive definite, so the optimization has a unique solution. The optimization can be efficiently solved using a proper solver. In the objective function, the quadratic term is designed to minimize the risk of spillover, while the linear term is intended to maximize the flow of traffic.

The proposed controller offers several features that enhance its implementation potential, compared to back-pressure approaches. First, the proposed controller takes into account several constraints inherent in practical traffic signal control systems, such as ensuring the minimum green duration for pedestrian safety. These constraints are incorporated into the optimization model, and the calculation of optimal signal control schemes is delegated to the optimizer. In contrast, back-pressure approaches may result in calculated control schemes that violate the constraints, lacking a systematic approach to finding sub-optimal solutions that satisfy all constraints. This makes the proposed controller more efficient and practical than conventional back-pressure approaches. Second, the proposed controller exhibits superior robustness, compared to back-pressure approaches by setting bounds on the maximum variation of green duration for each phase, thereby guaranteeing stable traffic flow. This characteristic is particularly valuable in the presence of significant traffic state estimation errors, which are inevitable when utilizing sparse trajectory data as the primary data source.

The detailed mechanism of the controller considers the following conditions.

1. $\exists p \in \mathcal{P}_n, v_p(k) < 0, h_p(k) \approx 0$. In this condition, for all the movements in the phase p, an upstream movement has the highest spillover risk as shown in Figure 3a. The variation of g_p has a negligible impact in reducing the value of the objective function. Therefore, the controller will give more green to the phase p as a larger g_p only marginally increases the objective, while decreasing the green duration of other phases can reduce the objective significantly. By increasing the green duration of the phase p, the outflow of the overlong queue will be increased, and the spillover risk will be reduced.

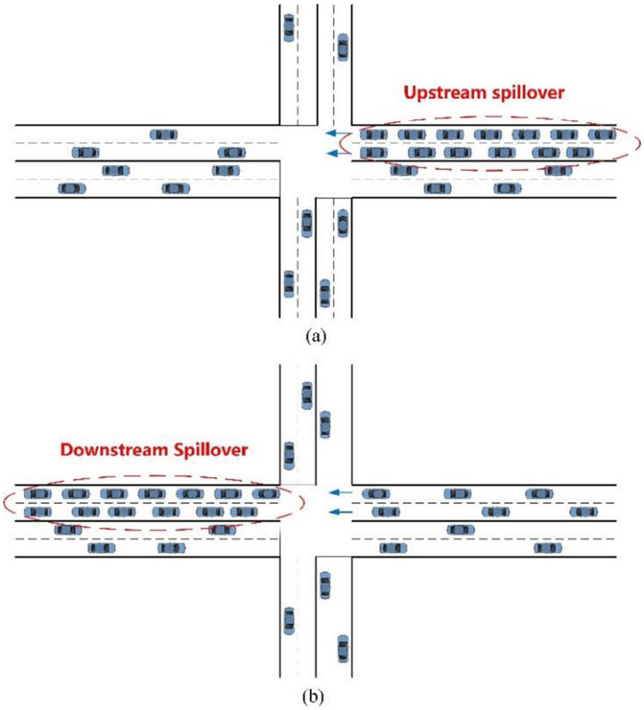

FIGURE 3 (a) An upstream movement has the highest spillover risk. (b) A downstream movement has the highest spillover risk.

2. $\forall p \in \mathcal{P}_n, v_p(k) < 0, h_p(k) \approx 0$. In this condition, every phase has a high upstream spillover risk. Therefore, the quadratic component in the objective function is close to 0, and the solution will be determined by the linear term. The linear term aims to maximize the flow, so it will give more green to the phases that have larger flow rates in the previous cycle.
3. $\exists p \in \mathcal{P}_n, v_p(k) > 0, h_p(k) > 1$, that is, a downstream movement has the highest spillover risk as shown in Figure 3b. In this condition, reducing g_p will result in a substantial reduction in the value of the objective function. Therefore, the optimizer will reduce the green of phase p and increase the green duration of other phases. If there exists another phase in which an upstream movement has the highest upstream spillover risk, the reduced green will be preferentially assigned to that phase.
4. $\forall p \in \mathcal{P}_n, h_p(k) > 1$, that is, every phase has a high downstream spillover risk. In this condition, the controller will reduce the green duration of the phases that have higher downstream spillover risks.

The proposed controller optimizes the signal of each intersection based on the estimated queue lengths of the upstream and downstream movement. Although queue length estimation for both freeways and urban intersections has been extensively investigated (Ghosh-Dastidar

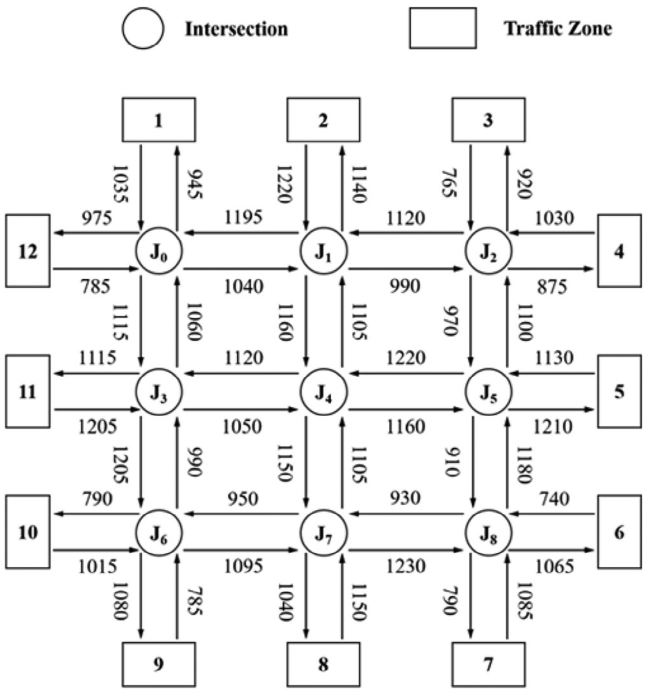

FIGURE 4 The topology of the synthetic traffic network.

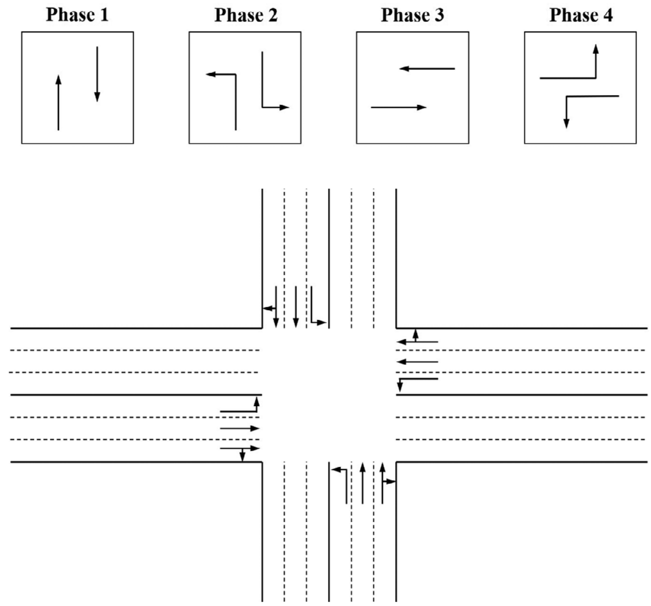

FIGURE 5 The geometric structure and phase sequence of each intersection.

& Adeli, 2006; Mei et al., 2019), in this paper, we solely employ a straightforward yet reliable method for estimating queue lengths. For movement m, the location of the most upstream queuing vehicle, $l_m(k)$, is represented by the position of the most upstream queuing CV in the last five cycles, that is, from cycle $k-5$ to $k-1$.

The proposed controller is switched on only when spillover risk exists. If all the movements of an intersection have no spillover risk, the proposed controller will be switched off, and the signal scheme of the intersection will be determined by the background signal control method.

3 | SIMULATION STUDY

In this section, the proposed signal control method is tested in microscopic simulation and compared with several baseline control methods. The simulation design and simulation results are presented in Sections 3.1 and 3.2, respectively.

3.1 | Simulation design

The proposed method is tested in a synthetic grid traffic network. The topology of the synthetic traffic network is shown in Figure 4. It contains 12 entering links and 12 exiting links, which directly connect to the origin zones and the destination zones shown in Figure 4. There are nine intersections and 48 links in the network. The length of every link is 480 m. For each intersection, it is assumed that every inroad consists of three lanes, comprising a dedicated left-turn lane, a straight lane, and a shared straight/right-turn lane. The geometric structure of each intersection is shown in Figure 5.

The traffic demand of each OD pair is shown in Table 3. It is assumed that all vehicles will select the shortest path to reach their respective destinations. The flow of each link is calculated by statically assigning the traffic demand to the network, and the results are illustrated in Figure 4. The proposed method is tested using the microscopic simulation software, SUMO (Lopez et al., 2018). In our simulation experiment, the Krauss model (Krauß, 1998), which is the default car-following model in SUMO, is applied as the underlying model to analyze the dynamics of the traffic system. The maximum speed is set to 50 km/h. The maximum acceleration and deceleration rates are set to 3.0 and −3.0 m/s^2, respectively. The desired (minimum) time headway for drivers is set to 1.25 s. The parameter that represents driver imperfection is set to 0.4 (0 denotes perfect driving). The length of each vehicle is set to 5 m, and the minimum length between vehicles is set to 2.5 m. All the vehicles depart from each origin are loaded instantaneously at the beginning of the simulation. If an entering link is too crowded, the vehicles are queued in the origin zone until it is possible to enter. This way, the traffic demand is loaded to the network with the maximum

TABLE 3 Traffic demand of each OD pair.

Origins \ Destinations	1	2	3	4	5	6	7	8	9	10	11	12
1	–	50	50	100	50	50	100	105	145	100	145	50
2	60	–	50	60	50	50	105	200	50	145	250	120
3	125	80	–	50	50	50	100	50	50	100	120	145
4	120	100	60	–	50	50	70	50	50	85	120	120
5	140	310	110	80	–	50	50	50	50	100	220	50
6	120	270	120	125	60	–	50	50	50	120	50	50
7	85	90	125	110	70	50	–	50	50	60	50	50
8	80	120	50	120	300	80	90	–	50	50	50	50
9	125	50	50	145	250	130	80	100	–	50	50	50
10	60	50	50	60	80	130	120	90	50	–	50	50
11	70	50	50	80	120	50	220	200	120	105	–	50
12	50	50	50	100	50	50	100	205	120	100	100	–

possible flow rates. The simulation stops after all the vehicles leave the network.

The following three control methods are tested in the simulation. It is assumed that the cycle length and the phase sequence of every signal control method are the same, and only the green splits are calculated by different methods. The common cycle length for every intersection is set to 80 s. The phase sequence of each intersection is shown in Figure 5. It is assumed that the right-turn movements are not controlled by traffic lights. The minimum and maximum green duration of a phase are set to 10 and 40 s, respectively. The maximum allowable variation of the green duration for a phase between consecutive cycles is set to 10 s. The three methods are tested using five different random seeds. Each seed configuration introduces randomness into the simulation, including factors like vehicle departure times, initial speeds, flow distributions, and the natural imperfections of drivers. The settings of those three control methods are briefly described as follows.

1. A fixed-time control method (Miller, 1963). The green duration of each phase is calculated based on the statically assigned flow of each movement. In this method, the movement of each phase that has the highest flow is the critical movement. The total green time is proportionally distributed to each phase based on the flow of its critical movement by the following equation,

$$g_p = G \cdot \frac{\max\limits_{m\in\mathcal{M}_p^n}\{q_m\}}{\sum_p \max\limits_{m\in\mathcal{M}_p^n}\{q_m\}} \tag{16}$$

where q_m is the flow of movement m. G is the total green time, which is the difference between the cycle length and the total lost time. The lost time of each phase is assumed to be 3 s. The calculated green duration of all the phases is summarized in Table 4.

TABLE 4 The signal scheme of the fixed-time control.

Intersection	Phase 1	Phase 2	Phase 3	Phase 4
J_0	16	19	20	13
J_1	23	13	22	10
J_2	18	14	16	20
J_3	22	10	21	15
J_4	18	16	19	15
J_5	23	10	24	11
J_6	21	13	16	18
J_7	21	16	21	10
J_8	17	18	21	12

2. Le's method. The green duration of each phase is calculated based on Equation (3). The parameter ϕ is set to 1 through the process of trial-and-error tuning. Note that the calculated signal control scheme may violate the constraints in Equations (10) and (11). If the calculated signal scheme violates the minimum green or the maximum green constraints, or the maximum variation of green duration, the signal scheme that is closest to the original scheme (which has the least root mean square deviation against the original scheme) will be applied.
3. The proposed method. The threshold queue length, r_c, is assigned a value of 0.75. For each intersection, the proposed controller is switched on only when spillover risk exists. If all the upstream and downstream movements of the intersection have no spillover risk, the proposed controller will be switched off, and the signal scheme of the intersection will be calculated by Le's

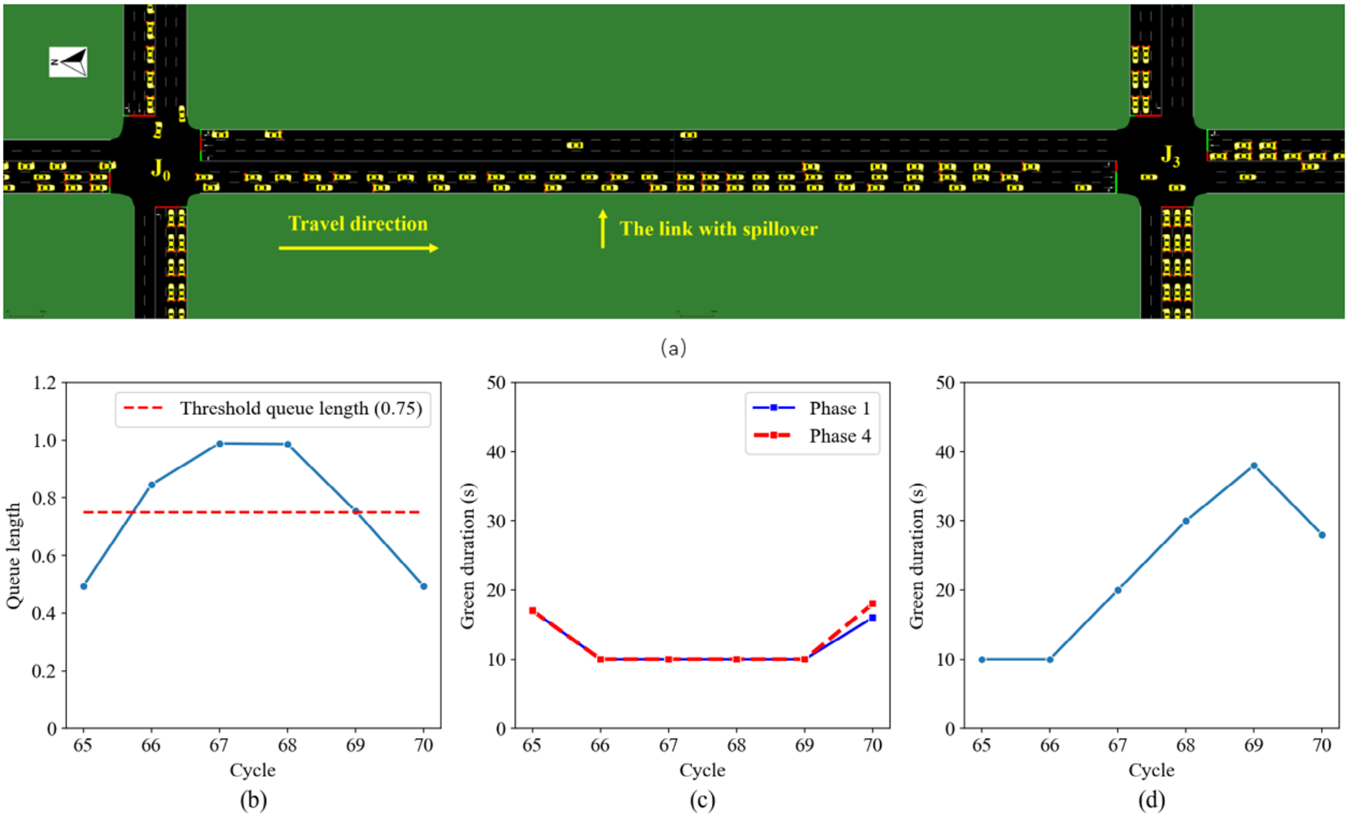

FIGURE 6 (a) An example of queue spillover, in which the queue length of the link that connects intersections J_0 and J_3 exceeds the threshold value. (b) The variation of queue length of the link between cycles 65 and 70. (c) The variations of green duration for phases 1 and 4 in intersection J_0. (d) The variation of green duration for phase 1 in intersection J_3.

method. The parameters μ and ϵ, are set to 15 and −0.01, respectively, through the process of trial-and-error tuning. The optimization is solved using the CVXOPT package in Python.

3.2 | Simulation results

First, we evaluate the performance of the proposed method by conducting evaluations with a CV penetration rate of 100%. Under this circumstance, it is assumed that there is no queue length estimation error. Figure 6 shows an example in which a queue spillover occurs on the link that connects intersections J_0 and J_3. For this link, the variation of queue length between cycles 65 and 70 is shown in Figure 6b. The queue length exceeds the threshold value at cycle 66. The proposed control method is activated at that control cycle for both intersections. Figure 6c shows the variation of green duration of phases 1 and 4 in the signal of the upstream intersection (J_0). The green duration of both phases is reduced at control cycle 66 and stays at the minimum value in the following cycles until the queue length falls below the threshold. The green reduction of those phases reduces the arrival flow of the overlong queue. Figure 6c shows the variation of green duration of phase 1 in the signal of the downstream intersection (J_3). The green duration of phase 1 increases during cycles 66–69, so the outflow of the overlong queue is increased. The queue length falls below the threshold after cycle 69, and the spillover is successfully mitigated.

As shown in the above example, once an overlong queue is identified, the proposed method optimizes the signals of the upstream and downstream intersections to reduce the inflow and increase the outflow, such that the overlong queue stops propagating further upstream.

The traffic performance of the network is quantified using different performance indicators as depicted in Figures 7 and 8. Within these figures, solid lines denote the averages of the performance indicators, while the shaded regions represent the corresponding standard deviations. Specifically, Figure 7 shows the number of overflowing links (the links that contain a queue longer than 0.95) in each control cycle for different control methods. In the proposed method, the number of overflowing links is significantly less than those observed in both the fixed-time control method and Le's method. The reason is that once an overlong queue occurs in the network, if no effective control action is implemented, the queue may soon

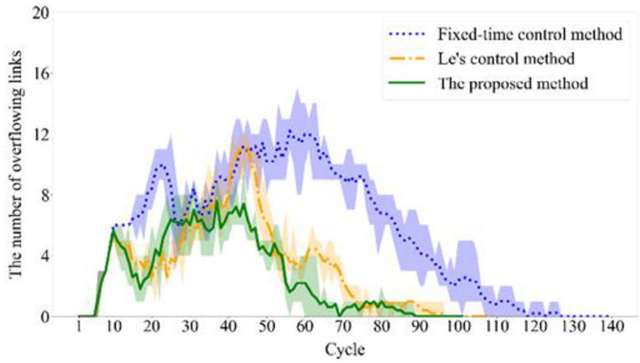

FIGURE 7 Comparison of the number of overflowing links among the three methods.

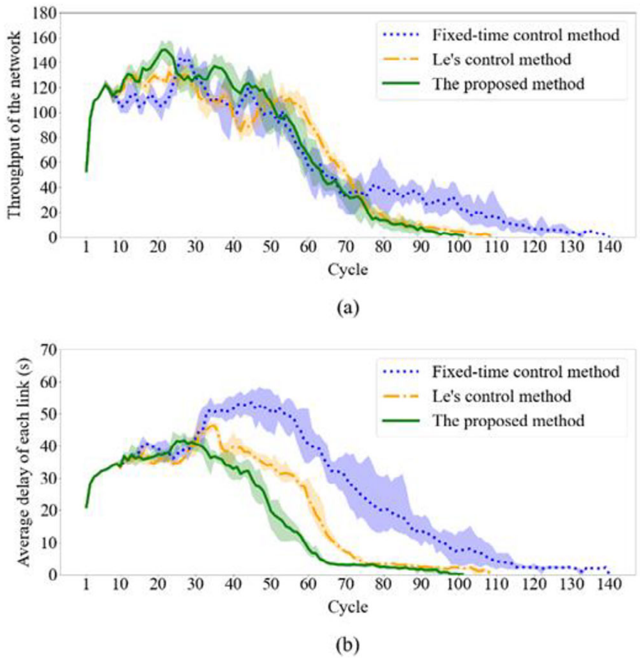

FIGURE 8 Performance comparison of the three methods: (a) The network throughput and (b) the average travel delay.

block the direct upstream intersection, leading to congestion propagating further upstream and consequently the increment of the number of overflowing links.

As discussed, spillovers may significantly reduce the throughput of the network. Figure 8a shows the comparison of the exit flow for different control methods. The proposed method achieves a higher network throughput than the fixed-time control method and Le's method during cycles 40–65, when spillovers frequently occur in the network. Therefore, it takes a much shorter time (about 100 cycles) for every vehicle to leave the network when applying the proposed method than applying the fixed-time control method (about 140 cycles) and Le's method (about 110 cycles). As a result, the proposed method achieves less travel delay than the other two methods as depicted in Figure 8b.

The MFD of a traffic network, as described by Geroliminis and Daganzo (2008), offers a straightforward means to evaluate the performance of a signal control strategy by depicting the relationship between the average occupancy and the total outflow (or average flow) of the network (Wu et al., 2011). Figure 9 shows the MFDs plotted with the simulation data in those three control scenarios. We have fitted a curve to the MFD obtained through the proposed method as illustrated in Figure 9c. This curve serves as a reference for comparing it to other baseline control methods. Figure 9a,b reveals that a significant portion of the MFD data points falls below the curve, indicating that the baseline methods result in inferior network traffic performance.

We further test the performance of the proposed method under different penetration rates of the CV, ranging from 1% to 100%. In the simulation, CVs are assumed to be randomly distributed in the traffic. The data updating frequency of the CVs is set to 3 s. The average travel time of all the vehicles achieved by the proposed method under different penetration rates is shown in Figure 10a. The proposed method performs the best when the penetration rate is 100% because there is no queue length estimation error. For lower penetration rates (e.g., from 2% to 10%), the proposed method still performs better than Le's control method with a 100% penetration rate of CVs. Only when the penetration rate is as low as 1%, the performance becomes inferior. Figure 10b shows the estimation errors (in terms of root mean square error) of queue length under different penetration rates. The error increases dramatically when the penetration rate is lower than 3%, causing the degradation of the proposed method.

Note that in this paper, we only use a very simple method to estimate the queue length. In the literature, there are more advanced methods of queue length estimation using trajectory data (Mei et al., 2019; Zhao et al., 2021), which may significantly improve the estimation accuracy. As those queue length estimation methods can be readily integrated into the proposed signal control method, the performance of the proposed method may be further improved in situations where the penetration rate of CV is significantly limited.

4 | REAL-WORLD IMPLEMENTATION

A field test experiment for the proposed method had been performed in a traffic network around the Beijing Capital International Airport. The geographical map of the traffic network is shown in Figure 11a. The proposed method had been implemented in 13 intersections, which are

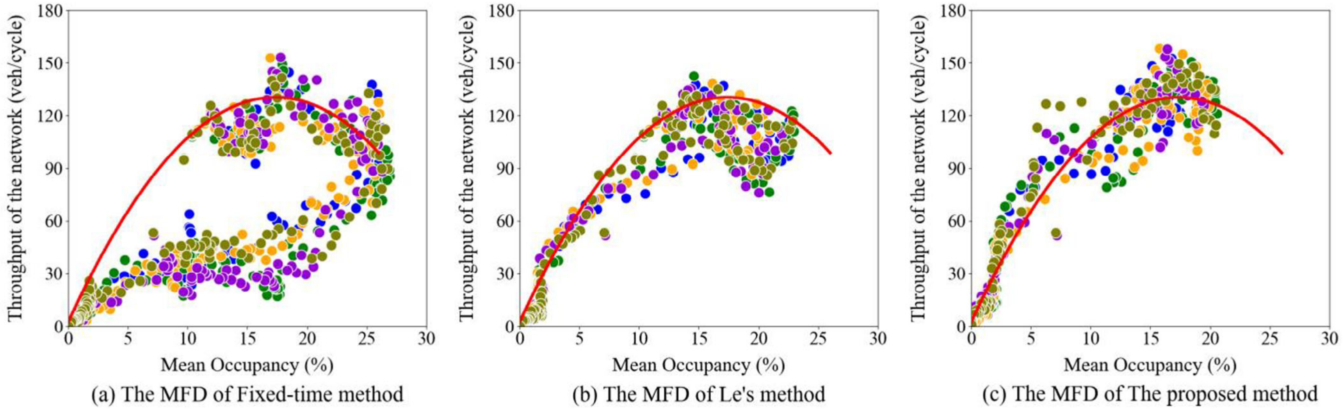

FIGURE 9 Macroscopic fundamental diagram (MFD) of (a) fixed-time control method, (b) Le's method, and (c) the proposed method. Each color represents the simulation results from a random seed.

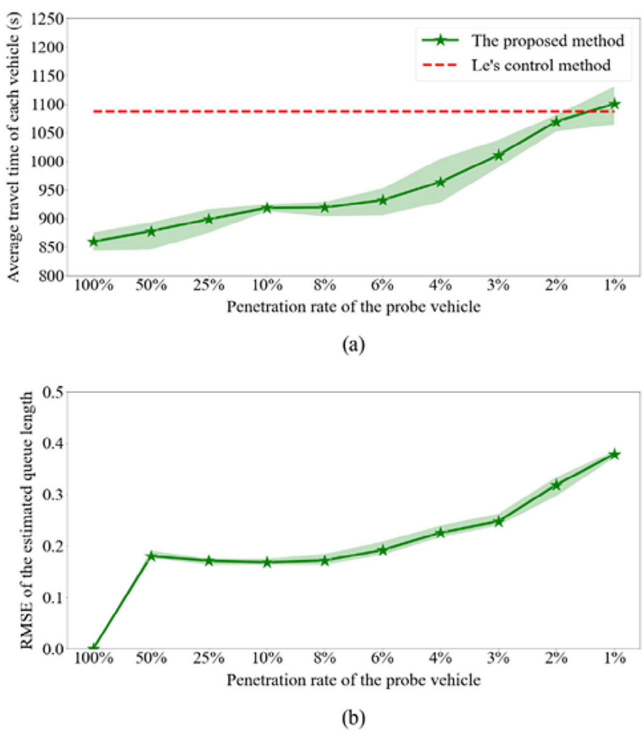

FIGURE 10 (a) The average travel time comparison and (b) the estimation errors of queue length under different CV penetration rates.

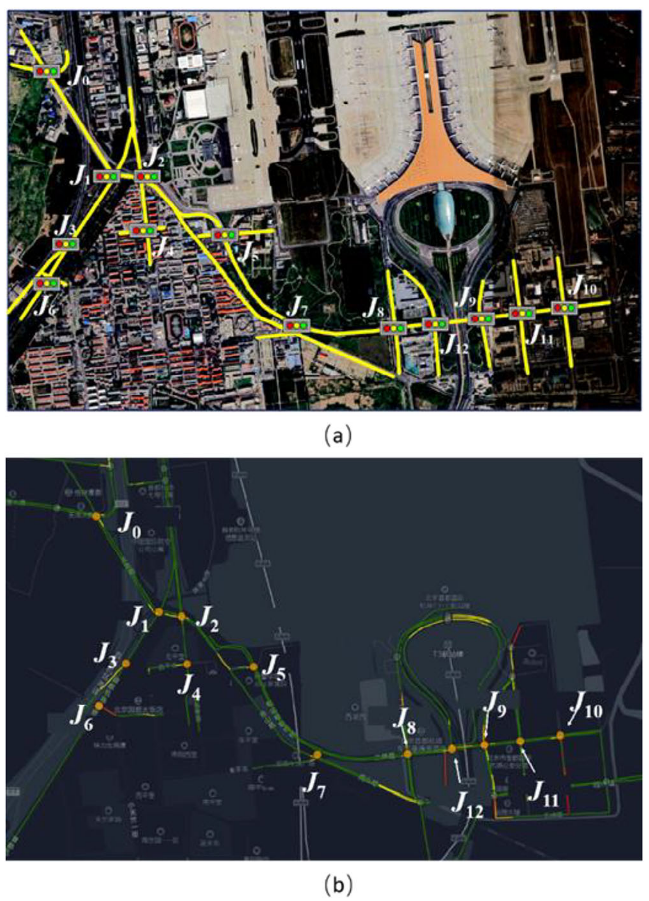

FIGURE 11 (a) The geographical map of the traffic network and (b) a screenshot from the visualization interface of the signal control system.

highlighted on the map. In this network, queue spillovers usually occurred at intersections J_1, J_2, J_7, J_8, J_9, and J_{12} in peak hours, resulting in high delays of the travelers. The proposed method was implemented into the online traffic signal control system developed by Didi smart transportation (Weili et al., 2020; Zheng & Liu, 2020). The traffic control system receives trajectory data acquired from CV and traffic control data from traffic signal controllers in real time. The data updating frequency of the CVs is 3 s. The data are processed and fed into the proposed control method to optimize the signal control scheme of each intersection. The system then provides optimized control schemes to the traffic signal controllers online for generating traffic control signals. A screenshot of the traffic network from the visualization interface of the control system is shown in Figure 11b.

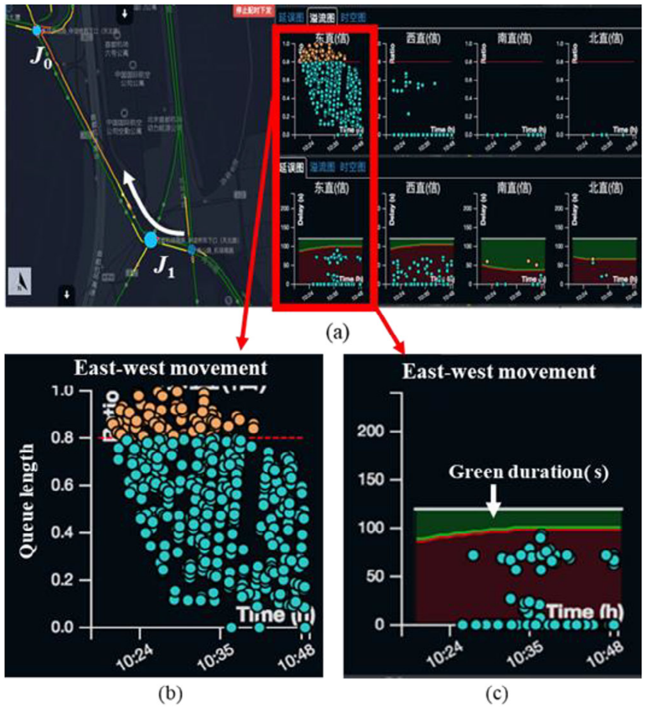

FIGURE 12 (a) The screenshots of an example in the field test experiment; (b) the queue length variation of the downstream link, in which spillover existed from 10:24 to 10:35 a.m.; and (c) the variation of the green duration (the width of the green strip) of the upstream signal.

The activation mechanism of the proposed method was the same as that in the simulation experiment, that is, the proposed method was activated only when spillover risk existed. In the absence of such risk, the intersection's signal plan was generated by an alternative online actuated traffic signal control method. In the testing site, the penetration rate of CVs was roughly estimated in the range between 5% and 10% based on manual on-site observations.

Figure 12 shows an example in which the proposed method successfully mitigated a queue spillover, which occurred at the downstream link of the highlighted movement (from east to west) of intersection J_1. Figure 12a is a screenshot from the visualization interface of the online traffic control system, where the captions of the figures were partially written in Chinese. The small figures enclosed by the red rectangle in Figure 12a show the variations of the downstream queue length and green duration of that movement. Those figures are edited by translating the Chinese characters into English as depicted in Figure 12b,c. In Figure 12b, each dot represents the queuing position of a CV relative to the length of the downstream link for that specific movement. The dots are displayed in yellow when the queuing position ratios exceed 0.8 and in blue otherwise. In

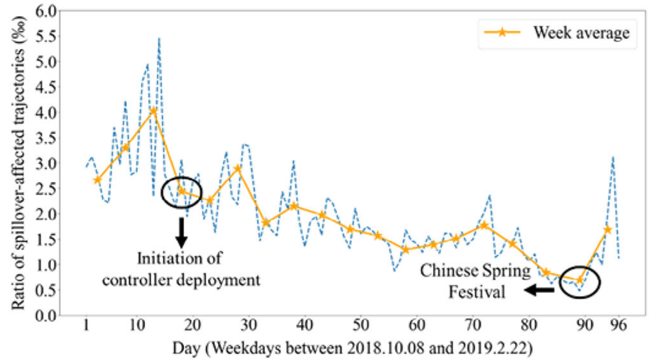

FIGURE 13 The variation of the ratio of spillover-affected trajectories before and after implementing the proposed control method.

Figure 12c, the width of the green and red strips represents the duration of the green and red phases for that movement.

In this example, queue spillover occurred around 10:20 a.m. when the queuing position ratios of many CVs exceeded 0.8. The controller consistently reduced the green duration of the movement until it reached the minimum value as depicted in Figure 12c. Gradually, the maximum queuing position of the CVs decreased and eventually fell below 0.8 after 10:35 a.m. This effective management successfully mitigated the spillover.

The proposed method had been tested between October 29, 2018, and February 22, 2019. We use two performance indicators to evaluate the proposed method. The first one is the ratio of spillover-affected trajectories. For each CV, the trajectory was labeled as spillover if there was a stop that occurred at a position further than 90% of the length of the link. The second is the spillover performance indicator (*SPI*) designed based on the following equation,

$$SPI = \frac{d^{spill} + 10 \times n_{stop}^{spill}}{3600} \tag{17}$$

where d^{spill} and n_{stop}^{spill} are the total travel delay and total number of stops of all the spillover-affected vehicles, respectively. We plotted the variations of these two performance indicators for all weekdays between October 8, 2018, and February 22, 2019, as depicted in Figures 13 and 14. Consequently, the data for the first 3 weeks (15 weekdays) in these figures represent the period without control implementation. Our analysis reveals a significant improvement after implementing the proposed method, with both the ratio of spillover-affected trajectories and the *SPI* showing substantial reductions. The average ratio of spillover-affected trajectories decreased by 49.3%, and the average *SPI* decreased by 39.3%.

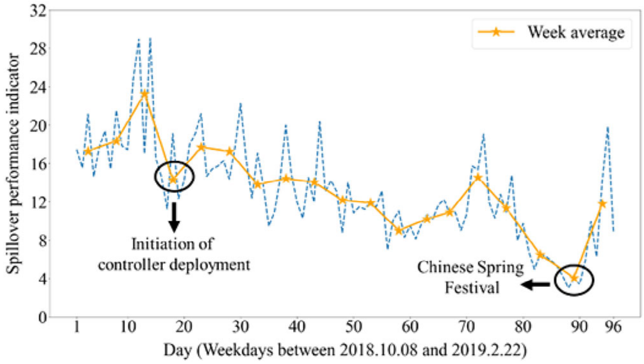

FIGURE 14 The variation of spillover performance indicator (*SPI*) before and after implementing the proposed control method.

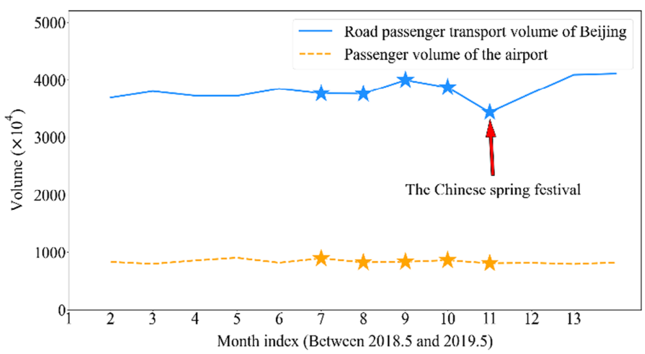

FIGURE 15 Monthly volumes of (a) road passenger transport volume data for Beijing and (b) the total passenger volume of the airport.

We observed a slight declining trend in the performance curves in Figures 13 and 14. This decline can be attributed to the continuous process of program debugging and parameter fine-tuning. Since our control method was directly applied in practice without initial parameter tuning through simulations, it required debugging and ongoing parameter refinement based on real-world feedback. This iterative process had the potential to enhance traffic performance.

To rule out the possibility that the improvement in traffic performance was due to variations in traffic demand, we obtained monthly road passenger transport volume data for Beijing and the total passenger volume of the airport from government websites as shown in Figure 15 (Beijing Capital International Airport Co., Ltd., 2018; Survey Office of the National Bureau of Statistics in Beijing, 2018). Our analysis of this mobility data indicated that there was no declining trend in monthly traffic volume during the testing period (highlighted using stars), with the exception of February, attributed to the Chinese Spring Festival. We have highlighted the data for the relevant weeks in Figures 13 and 14.

5 | CONCLUSION AND DISCUSSIONS

This paper proposes a real-time traffic signal control method based on trajectory data obtained from CVs. The proposed method optimizes the green splits of each intersection's signal to prevent queue spillovers. The signal control problem is tackled by formulating it as a computationally efficient linear quadratic optimization model. The proposed method is designed for the prevalent fixed cyclic signal control mode. It also incorporates many constraints in practical traffic signal control systems.

The effectiveness of the proposed method has been verified through both simulation experiments and field test experiments. In the simulation experiment, the proposed method outperforms several existing signal control methods, including a fixed-time control method and a back-pressure-based method, in preventing queue spillovers and reducing travel delays reducing spillover even with a penetration rate as low as 5%. In the field test experiment, the proposed method had been tested in a traffic network including 13 intersections. The performance has been evaluated based on crowd-sourced vehicles' trajectory data by using two performance indicators, which both represent the severity of queue spillovers. Both indicators were significantly reduced after implementing the proposed method.

For future research, we will consider to integrate the proposed distributed signal control method with a coordinated signal control method to further improve traffic performance. While the proposed method effectively prevents spillover by adjusting the direct upstream and downstream signals of critical movements, it remains responsive. By coordinating signals at further upstream and downstream intersections, we aim to proactively reduce spillover risks. This will involve incorporating traveler routing information and increasing computational complexity. We will focus on developing a coordinated signal control method that can efficiently manage this complexity while maintaining a real-time implementable computation time. Furthermore, the implementation of the proposed method still follows a centralized approach, necessitating a traffic management center for data collection and control decisions. As V2V and V2X communications advance, leveraging edge computing for decentralized deployment could further enhance the scalability of the signal control method. This avenue will also be investigated in future research.

REFERENCES

Beijing Capital International Airport Co., Ltd. (2018). *Airport operation data by year*. Beijing Capital International Airport Co., Ltd. https://en.bcia.com.cn/yysj.html

Daganzo, C. F. (1998). Queue spillovers in transportation networks with a route choice. *Transportation Science*, *32*(1), 3–11.

Ding, C., Dai, R., Fan, Y., Zhang, Z., & Wu, X. (2022). Collaborative control of traffic signal and variable guiding lane for isolated intersection under connected and automated vehicle environment. *Computer-Aided Civil and Infrastructure Engineering*, *37*(15), 2052–2069.

Dixit, V., Nair, D. J., Chand, S., & Levin, M. W. (2020). A simple crowdsourced delay-based traffic signal control. *PLoS ONE*, *15*(4), e0230598.

Geroliminis, N., & Daganzo, C. F. (2008). Existence of urban-scale macroscopic fundamental diagrams: Some experimental findings. *Transportation Research Part B: Methodological*, *42*(9), 759–770.

Geroliminis, N., Haddad, J., & Ramezani, M. (2012). Optimal perimeter control for two urban regions with macroscopic fundamental diagrams: A model predictive approach. *IEEE Transactions on Intelligent Transportation Systems*, *14*(1), 348–359.

Geroliminis, N., & Sun, J. (2011). Properties of a well-defined macroscopic fundamental diagram for urban traffic. *Transportation Research Part B: Methodological*, *45*(3), 605–617.

Ghosh-Dastidar, S., & Adeli, H. (2006). Neural network-wavelet microsimulation model for delay and queue length estimation at freeway work zones. *Journal of Transportation Engineering*, *132*(4), 331–341.

Gregoire, J., Qian, X., Frazzoli, E., De La Fortelle, A., & Wongpiromsarn, T. (2014). Capacity-aware backpressure traffic signal control. *IEEE Transactions on Control of Network Systems*, *2*(2), 164–173.

Han, Y., Hegyi, A., Yuan, Y., Roncoli, C., & Hoogendoorn, S. (2018). An extended linear quadratic model predictive control approach for multi-destination urban traffic networks. *IEEE Transactions on Intelligent Transportation Systems*, *20*(10), 3647–3660.

Han, Y., Wang, M., & Leclercq, L. (2023). Leveraging reinforcement learning for dynamic traffic control: A survey and challenges for field implementation. *Communications in Transportation Research*, *3*, 100104.

Hunt, P., Robertson, D., Bretherton, R., & Royle, M. C. (1982). The SCOOT on-line traffic signal optimisation technique. *Traffic Engineering & Control*, *23*(4), 190–192.

Jiang, X., & Adeli, H. (2004). Object-oriented model for freeway work zone capacity and queue delay estimation. *Computer-Aided Civil and Infrastructure Engineering*, *19*(2), 144–156.

Karim, A., & Adeli, H. (2003). Fast automatic incident detection on urban and rural freeways using wavelet energy algorithm. *Journal of Transportation Engineering*, *129*(1), 57–68.

Krauß, S. (1998). *Microscopic modeling of traffic flow: Investigation of collision free vehicle dynamics* [Doctoral dissertation, University of Cologne, Köln].

Le, T., Kovács, P., Walton, N., Vu, H. L., Andrew, L. L., & Hoogendoorn, S. (2015). Decentralized signal control for urban road networks. *Transportation Research Part C: Emerging Technologies*, *58*, 431–450.

Le, T., Vu, H. L., Nazarathy, Y., Vo, Q. B., & Hoogendoorn, S. (2013). Linear-quadratic model predictive control for urban traffic networks. *Transportation Research Part C*, *36*, 498–512.

Levin, M. W. (2023). Max-pressure traffic signal timing: A summary of methodological and experimental results. *Journal of Transportation Engineering, Part A: Systems*, *149*(4), 03123001.

Levin, M. W., Hu, J., & Odell, M. (2020). Max-pressure signal control with cyclical phase structure. *Transportation Research Part C: Emerging Technologies*, *120*, 102828.

Li, D., Wu, J., Zhu, F., Chen, T., & Wong, Y. D. (2023). Modeling adaptive platoon and reservation-based intersection control for connected and autonomous vehicles employing deep reinforcement learning. *Computer-Aided Civil and Infrastructure Engineering*, *38*(10), 1346–1364.

Li, L., & Jabari, S. E. (2019). Position weighted backpressure intersection control for urban networks. *Transportation Research Part B: Methodological*, *128*, 435–461.

Lopez, P. A., Behrisch, M., Bieker-Walz, L., Erdmann, J., Flötteröd, Y.-P., Hilbrich, R., Lücken, L., Rummel, J., Wagner, P., & Wießner, E. (2018). Microscopic traffic simulation using sumo. *2018 21st International Conference on Intelligent Transportation Systems (ITSC)*, Big Island, HI (pp. 2575–2582).

Lowrie, P. (1982). The Sydney Coordinated Adaptive Traffic System: Principles, methodology, algorithms. *International Conference on Road Traffic Signalling*, London, UK.

Ma, C., Yu, C., Zhang, C., & Yang, X. (2023). Signal timing at an isolated intersection under mixed traffic environment with self-organizing connected and automated vehicles. *Computer-Aided Civil and Infrastructure Engineering*, *38*(14), 1955–1972.

Ma, D., Xiao, J., Song, X., Ma, X., & Jin, S. (2020). A back-pressure-based model with fixed phase sequences for traffic signal optimization under oversaturated networks. *IEEE Transactions on Intelligent Transportation Systems*, *22*(9), 5577–5588.

Mei, Y., Gu, W., Chung, E. C., Li, F., & Tang, K. (2019). A Bayesian approach for estimating vehicle queue lengths at signalized intersections using probe vehicle data. *Transportation Research Part C: Emerging Technologies*, *109*, 233–249.

Mercader, P., Uwayid, W., & Haddad, J. (2020). Max-pressure traffic controller based on travel times: An experimental analysis. *Transportation Research Part C: Emerging Technologies*, *110*, 275–290.

Miller, A. J. (1963). Settings for fixed-cycle traffic signals. *Journal of the Operational Research Society*, *14*(4), 373–386.

Papageorgiou, M., Diakaki, C., Dinopoulou, V., Kotsialos, A., & Wang, Y. (2003). Review of road traffic control strategies. *Proceedings of the IEEE*, *91*(12), 2043–2067.

Peng, B., Keskin, M. F., Kulcsár, B., & Wymeersch, H. (2021). Connected autonomous vehicles for improving mixed traffic efficiency in unsignalized intersections with deep reinforcement learning. *Communications in Transportation Research*, *1*, 100017.

Shi, H., Nie, Q., Fu, S., Wang, X., Zhou, Y., & Ran, B. (2022). A distributed deep reinforcement learning–based integrated dynamic bus control system in a connected environment. *Computer-Aided Civil and Infrastructure Engineering*, *37*(15), 2016–2032.

Shi, H., Zhou, Y., Wang, X., Fu, S., Gong, S., & Ran, B. (2022). A deep reinforcement learning-based distributed connected automated vehicle control under communication failure. *Computer-Aided Civil and Infrastructure Engineering*, *37*(15), 2033–2051.

Survey Office of the National Bureau of Statistics in Beijing. (2018). Survey Office of the National Bureau of Statistics in Beijing. https://tjj.beijing.gov.cn/tjsj_31433/yjdsj_31440/ysyd_31830/

Van den Berg, M., Hegyi, A., De Schutter, B., & Hellendoorn, J. (2007). Integrated traffic control for mixed urban and freeway networks: A model predictive control approach. *European Journal of Transport and Infrastructure Research*, *7*(3), 223–250.

Varaiya, P. (2013). The max-pressure controller for arbitrary networks of signalized intersections. In A. Ukkusuri & K. Ozbay (Eds.), *Advances in dynamic network modeling in complex transportation systems* (pp. 27–66). Springer.

Wang, X., Yin, Y., Feng, Y., & Liu, H. X. (2022). Learning the max pressure control for urban traffic networks considering the phase switching loss. *Transportation Research Part C: Emerging Technologies*, *140*, 103670.

Wei, H., Chen, C., Zheng, G., Wu, K., Gayah, V., Xu, K., & Li, Z. (2019). PressLight: Learning max pressure control to coordinate traffic signals in arterial network. *Proceedings of the 25th ACM SIGKDD International Conference on Knowledge Discovery & Data Mining*, Anchorage, AK (pp. 1290–1298).

Weili, S., Liu, X., Zheng, J., & Jinqing, Z. (2020). *Systems and methods for controlling traffic lights* (U.S. Patent No. 10,600,320). Google Patents. https://patents.google.com/patent/US10600320B2/en

Wongpiromsarn, T., Uthaicharoenpong, T., Wang, Y., Frazzoli, E., & Wang, D. (2012). Distributed traffic signal control for maximum network throughput. *2012 15th International IEEE Conference on Intelligent Transportation Systems*, Anchorage, AK (pp. 588–595).

Wu, X., Liu, H. X., & Geroliminis, N. (2011). An empirical analysis on the arterial fundamental diagram. *Transportation Research Part B: Methodological*, *45*(1), 255–266.

Wunderlich, R., Elhanany, I., & Urbanik, T. (2007). A stable longest queue first signal scheduling algorithm for an isolated intersection. *2007 IEEE International Conference on Vehicular Electronics and Safety*, Beijing, China (pp. 1–6).

Xiao, N., Frazzoli, E., Li, Y., Luo, Y., Wang, Y., & Wang, D. (2015). Further study on extended back-pressure traffic signal control algorithm. *2015 54th IEEE Conference on Decision and Control (CDC)*, Osaka, Japan (pp. 2169–2174).

Xu, Q., Li, K., Wang, J., Yuan, Q., Yang, Y., & Chu, W. (2022). The status, challenges, and trends: An interpretation of technology roadmap of intelligent and connected vehicles in China (2020). *Journal of Intelligent and Connected Vehicles*, *5*(3), 1–7.

Zhang, Z., Guo, M., Fu, D., Mo, L., & Zhang, S. (2022). Traffic signal optimization for partially observable traffic system and low penetration rate of connected vehicles. *Computer-Aided Civil and Infrastructure Engineering*, *37*(15), 2070–2092.

Zhao, Y., Wong, W., Zheng, J., & Liu, H. X. (2021). Maximum likelihood estimation of probe vehicle penetration rates and queue length distributions from probe vehicle data. *IEEE Transactions on Intelligent Transportation Systems*, *23*(7), 7628–7636.

Zheng, J., & Liu, X. (2020). *Adaptive traffic control using vehicle trajectory data* (U.S. Patent No. 10,629,071). Google Patents. https://patents.google.com/patent/US10629071B1/en

How to cite this article: Han, Y., Han, Z., Ding, F., Li, F., Wang, H., & Wang, X. (2023). Field-tested signal controller to mitigate spillover using trajectory data. *Computer-Aided Civil and Infrastructure Engineering*, 1–16. https://doi.org/10.1111/mice.13144